ANL-78-16

ADVANCED FUEL CELL DEVELOPMENT

Progress Report for October—December 1977

by

J. P. Ackerman, Kimio Kinoshita, P. A. Finn,
J. W. Sim, and P. A. Nelson

ARGONNE NATIONAL LABORATORY, ARGONNE, ILLINOIS

Prepared for the U. S. DEPARTMENT OF ENERGY
under Contract W-31-109-Eng-38

Printed in the United States of America
Available from
National Technical Information Service
U. S. Department of Commerce
5285 Port Royal Road
Springfield, Virginia 22161
Price: Printed Copy $4.50; Microfiche $3.00

Distribution Category:
Energy Conversion
(UC-93)

ANL-78-16

ARGONNE NATIONAL LABORATORY
9700 South Cass Avenue
Argonne, Illinois 60439

ADVANCED FUEL CELL DEVELOPMENT

Progress Report for
October—December 1977

by

J. P. Ackerman, Kimio Kinoshita, P. A. Finn,
J. W. Sim, and P. A. Nelson

Chemical Engineering Division

March 1978

Previous Reports in this Series

ANL-77-29	January—March 1977
ANL-77-56	April—June 1977
ANL-77-79	July—September 1977

TABLE OF CONTENTS

LIST OF FIGURES

LIST OF TABLES

CHEMICAL ENGINEERING DIVISION

ADVANCED FUEL CELL DEVELOPMENT

October—December 1977

by

J. P. Ackerman, Kimio Kinoshita, P. A. Finn,
J. W. Sim, and P. A. Nelson

ABSTRACT

This report describes advanced fuel cell research and development activities at Argonne National Laboratory (ANL) during the period October-December 1977. This work has been aimed at understanding and improving the performance of fuel cells having molten alkali-carbonate mixtures as electrolytes; the fuel cells operate at temperatures near 925 K. The largest part of this effort has been directed toward development of methods for fabricating and evaluating electrolyte structures for these cells. Cell performance, life, and cost are the criteria of optimization. During this quarter, the desirable physical characteristics of $LiAlO_2$ particles, which act to retain the molten carbonates in the electrolyte structure of the cell, have been more clearly defined; a low temperature synthesis of the stable γ-allotrope of $LiAlO_2$ has been devised; an extensive study of $LiAlO_2$ stability has begun; and analytical methods have been refined for separating $LiAlO_2$, in unaltered form, from carbonates. Testing of various electrolyte structures and other components in 7-cm-dia round cells has provided a means for evaluating new electrolyte developments and verifying a previously developed method for protecting the wet-seal areas of a cell from corrosion.

SUMMARY

Electrolyte Development

Preparation and Characterization of Electrolytes. An attractive low-temperature (725 K) synthesis of the γ-allotrope of $LiAlO_2$ was devised. This method represents a possible route to the production of high-surface-area, thermally stable $LiAlO_2$. Synthesis and testing of electrolyte structures (tiles) containing controlled amounts of several $LiAlO_2$ particle types (different size ranges and shapes) has shown the need for a high fraction of fine $LiAlO_2$ particles in the electrolyte tile. The synthesis of $LiAlO_2$ from low-cost aluminas, which was first reported last quarter, has been extended to yield several different particle sizes and shapes; prospects are excellent for ultimately using alumina of very low cost to produce $LiAlO_2$ for commercial cells.

Physical Stability of $LiAlO_2$. A major effort is under way to determine the physical stability of $LiAlO_2$ under various conditions which may exist in operating cells. The γ-allotrope of $LiAlO_2$ appears to be the most stable of the three allotropes (α, β, and γ) in short-term tests at temperatures near the high end of the range expected in operating cells. The effects of temperature and gas environment (CO_2, $H_2/CO_2/H_2O$, and air) on all three allotropic forms are under study; this work will be extended to long-term tests.

Chemical Stability of $LiAlO_2$. An improved method, namely, treatment with 38 vol % glacial acetic acid/62 vol % acetic anhydride, for isolating $LiAlO_2$ from the carbonates in the electrolyte tile does not appear to affect the allotropic distribution, and high recoveries are obtained. Aqueous dissolution in 6*M* HCl selectively removes the β- and γ-allotropes. No chemical change in $LiAlO_2$ is detectable upon heating in air, with carbonates, until the temperature reaches $\sim$1100 K ($\sim$200 K above nominal cell operating temperature); at this temperature γ-$LiAlO_2$ begins to decompose to form Li_5AlO_4.

Cell Testing

Operation of cells having electrolyte tiles produced from several controlled mixtures of $LiAlO_2$ particle types has verified the need for tiles containing a large fraction of small $LiAlO_2$ particles. Cell performance was directly related to the amount of $LiAlO_2$ present as fine particles, and physical strength of the tile appeared to be similarly correlated. Minor refinements were made in the method of application of an aluminizing coating to provide corrosion protection to the wet-seal area of the cell. This method continues to give good protection and appears to be of acceptable cost.

I. INTRODUCTION

The advanced fuel cell studies at Argonne National Laboratory (ANL) are part of the DOE Second Generation Fuel Cell Program. The goal of this DOE program is the earliest possible introduction of high-efficiency generating systems based on molten-carbonate fuel cells, which have the capability of operating on coal or other fuels. At the present stage of development, the primary thrust of the program is directed to development of the fuel cell itself.

A molten carbonate fuel cell consists of a porous metal anode (presently nickel or an alloy of nickel), a porous nickel oxide cathode, an electrolyte structure which separates the anode and cathode and conducts only ionic current between them, and appropriate metal housings or, in the case of stacks of cells, intercell separator plates. The cell housings (or separator plates) bear upon the electrolyte structure to form a seal between the environment and the anode and cathode gas compartments. The electrolyte structure, which is commonly called a "tile," is a composite structure of solid $LiAlO_2$ particles and a mixture of alkali metal carbonates which are liquid at the cell operating temperature of 925 K. At the anode, hydrogen and carbon monoxide in the fuel gas react with carbonate ion from the electrolyte to form carbon dioxide and water, giving up electrons to the external circuit. At the cathode, carbon dioxide and oxygen react and accept electrons from the external circuit to re-form carbonate ion, which is conducted through the electrolyte to the anode. In a practical cell stack, CO_2 for the cathode would be obtained from the anode exhaust.

The ANL contribution to the program is intended to provide understanding of cell behavior and to develop improved components and processes. More improvements are needed in the electrolyte tile than in any other single component. For this reason, electrolyte development is receiving special attention at ANL. Characterization of tile properties and the relation of the properties to tile behavior in cells is of major importance. Determination of the stability of tile materials is also of high priority.

Operation of cells is required for assessment of the behavior of tiles and other components and for understanding of the performance and life-limiting mechanisms at work within the cell. Cell operation is, of course, coupled with a diagnostic effort and a materials-development effort, with the aim of developing cells of adequate performance and longevity for realistic component testing.

II. ELECTROLYTE DEVELOPMENT

A. Preparation and Characterization of Electrolytes

In the molten-carbonate fuel cell, the carbonate electrolyte is held in a matrix of unconsolidated lithium aluminate particles by surface forces. The shape and size distribution of the lithium aluminate particles in this electrolyte structure (tile) have a significant effect on the performance and life of the cells. For this reason, the molten-carbonate fuel cell research and development effort at Argonne has focused on the synthesis and characterization of electrolyte tiles and their effect on fuel-cell performance. A major part of this effort has been directed towards the synthesis of lithium aluminate particles with well-defined shapes and submicrometer sizes by economical techniques. At the same time, the feasibility of using low-cost alumina in the synthesis of lithium aluminate is being examined. A variety of aluminas are commercially available having costs less than one tenth that of Degussa Type C alumina, the type commonly used in synthesis of lithium aluminate for fuel cells.

Effort during this quarter was centered on producing mixtures of high-surface-area, clump-shaped $LiAlO_2$ and low-surface-area, rod-shaped $LiAlO_2$ in alkali carbonate matrices. (The rod-shaped particles should enhance the mechanical strength of the tile, whereas the smaller, clump-shaped particles are needed for good electrolyte retention.) Electrolyte tiles prepared from these mixtures were tested in 7-cm-dia fuel cells.

Table 1 summarizes the procedures used to prepare the electrolyte mixtures containing clump- and rod-shaped $LiAlO_2$, as well as the procedures previously used to prepare α-$LiAlO_2$ in the form of clumps, and β-$LiAlO_2$ in the form of rods. Also presented in the table are results of scanning electron microscopy (SEM) and X-ray diffraction* analyses performed to characterize the products. All of the procedures yielded products containing 55 wt % alkali carbonates (62 mol % Li_2CO_3-38 mol % K_2CO_3). In the procedures used previously, α-$LiAlO_2$ was prepared by heating powders of Li_2CO_3-K_2CO_3 and γ-Al_2O_3 in CO_2 at 875 K for 24 h, whereas β-$LiAlO_2$ was prepared by impregnating γ-Al_2O_3 with LiOH-KOH and heating this material in CO_2, first at 295 K to form $LiAlO_2$ and then at 725 K to convert unreacted hydroxides to carbonates and to remove water. In the new procedure, powders of Li_2CO_3, K_2CO_3, γ-Al_2O_3, LiOH, and KOH were heated in CO_2 at 295 K to form rod-shaped β-$LiAlO_2$ by reaction of γ-Al_2O_3 with hydroxides and then at a higher temperature (775 or 875 K) to convert unreacted hydroxides to carbonates, remove water, and form α-$LiAlO_2$ by reaction of γ-Al_2O_3 with carbonates. The relative amounts of rod- and clumped-shaped particles of $LiAlO_2$ in the electrolyte mixtures were controlled by the proportions of hydroxides and carbonates in the starting material (columns 3 and 4, Table 1).

Examination of the two mixed products by SEM clearly showed that both clump- and rod-shaped particles were present after CO_2 treatments at 295 K and 775 (or 875) K, as shown in Table 1. Furthermore, the relative amounts of clumps and rods appeared proportional to the weight ratios of the starting

---

*All X-ray diffraction analyses described in this report were performed by B. S. Tani, Analytical Chemistry Laboratory, ANL.

Table 1. Preparation of $LiAlO_2$-Electrolyte Mixtures

Starting Materials[a]		Weight Fraction		Treatment of Mixture[b]				
Powder 1[c]	Powder 2[d]	Powder 1	Powder 2	Temp., K	Time, h	SEM Results	X-ray Diffraction Results	Fuel Cell Test
Li_2CO_3-K_2CO_3/γ-Al_2O_3	--	1.0	--	875	24	clumps	α-$LiAlO_2$	CS-7
Li_2CO_3-K_2CO_3/γ-Al_2O_3	LiOH-KOH/γ-Al_2O_3	0.8	0.2	295 875	4 3	rods, clumps	β-$LiAlO_2$ (major) α-$LiAlO_2$ (minor)	CS-11
Li_2CO_3-K_2CO_3/γ-Al_2O_3	LiOH-KOH/γ-Al_2O_3	0.5	0.5	295 775	5 2.5	rods, clumps	β-$LiAlO_2$ (major) α-$LiAlO_2$ (minor)	CS-9
--	LiOH-KOH/γ-Al_2O_3	--	1.0	295 725	7 7.5	rods	β-$LiAlO_2$	CS-4

[a] The γ-Al_2O_3 used was Degussa Type C.

[b] Samples heated in CO_2.

[c] 0.60 Li_2CO_3 + 0.16 K_2CO_3 + 0.33 γ-Al_2O_3.

[d] 3.8 LiOH + 1.3 KOH + 0.98 γ-Al_2O_3.

materials, *i.e.*, a 1:1 ratio of powders 1 and 2 produced a 1:1 ratio of clumps and rods and a 4:1 ratio of these powders produced a 4:1 ratio of clumps and rods. The SEM results were not in agreement with the X-ray diffraction results, which are also shown in Table 1. We believe that this anomaly is due to the small crystallite size (<0.1 μm) of the α-$LiAlO_2$, which decreases the intensity of lines in the α-$LiAlO_2$ X-ray diffraction pattern. Therefore, the SEM results were judged to be more representative of the relative amounts of clumps and rods present in the mixtures.

The search was continued for a low-cost substitute for Degussa Type C γ-Al_2O_3, the material generally used in the synthesis of $LiAlO_2$. In recent work, ALCOA* Type F-1 alumina was tested. The cost of this material, $0.50/kg ($0.225/lb) in bulk quantities (19,000-kg shipment), is about 13 times lower than that of Degussa Al_2O_3. X-ray diffraction analyses indicated that the F-1 material was γ-AlOOH (boehmite), a hydrated alumina. The surface area† reported by the manufacturer for this material is 210 m^2/g, as compared with 100 ± 15 m^2/g for Degussa Type C.

Since γ-AlOOH is used industrially as a drying agent, the major fraction of its surface area is probably associated with micropores in the γ-AlOOH particles. The loose bulk density of γ-AlOOH is 0.83 g/cm^3 (52 lb/ft^3), a value that is considerably higher than that of Degussa γ-Al_2O_3, 0.06 g/cm^3 (4 lb/ft^3). These values suggest that the average particle size of γ-AlOOH is larger than that of Degussa γ-Al_2O_3 even though γ-AlOOH has a higher surface area. In physical mixtures of LiOH and γ-Al_2O_3 or γ-AlOOH, the rate of reaction to form $LiAlO_2$ is a function of the particle size of the starting material and, hence, Degussa γ-Al_2O_3 is expected to react more rapidly than γ-AlOOH.

An experiment to synthesize rod-shaped particles of $LiAlO_2$ using ALCOA γ-AlOOH was conducted as follows. A slurry of γ-AlOOH in LiOH and KOH solution was heated to remove H_2O, and the dry powder was exposed to flowing CO_2 at 295 K for 8 h and then at 675 K for 4.5 h. X-ray diffraction analyses showed that the β-$LiAlO_2$ was the major phase, and SEM examinations showed that the particles were rods and needles. The rodlike particles were about 0.5 μm in diameter and about 1-2 μm long, and the needles were <0.1 μm in diameter and <0.5 μm long. The rod-shaped particles of β-$LiAlO_2$ have dimensions similar to those of rod-shaped $LiAlO_2$ obtained previously from starting materials of Degussa Al_2O_3 (ANL-77-29, pp. 4-11) or from ALCOA $Al_2O_3 \cdot 3H_2O$, Type C-33 (ANL-77-79, p. 4). The needles have never been observed before; therefore, the synthesis with γ-AlOOH will be repeated to see whether the needles can be reproduced. If the synthesis is successful, needle-containing material will be used to make tiles which will be evaluated in actual fuel cells.

Alternative approaches based on the reaction of LiOH and Al_2O_3 were also investigated, with the aim of obtaining high-surface-area $LiAlO_2$ with particle shapes other than rods. In one approach, Al_2O_3 was physically mixed with or impregnated with LiOH, then heated in air. In another approach, Al_2O_3 was mixed with LiOH, Li_2CO_3, and K_2CO_3 before heating in air.

---

* Aluminum Company of America.

† Determined by the Brunauer, Emmett, and Teller (BET) method.

Table 2 summarizes the results of experiments in which LiOH and Al_2O_3 were heated together in air. Samples 27, 39A, and 66A were made from physical mixtures of LiOH (sieved to <63 μm) and Al_2O_3. Sample 27 contained a two-fold excess of LiOH over that required for the stoichiometric conversion of Al_2O_3 to $LiAlO_2$, whereas samples 39A, 66A, and 65 contained stoichiometric amounts of LiOH and Al_2O_3. Sample 65 was prepared by impregnating γ-AlOOH with LiOH from aqueous solution. The drying step was carried out at 435 K, where a partial conversion of γ-AlOOH to β-$LiAlO_2$ occurred. X-ray diffraction analyses of the four $LiAlO_2$ products shown in Table 2, obtained after heating at 725 K, showed only the presence of the β-allotrope. The SEM analyses showed that, in general, the β-$LiAlO_2$ particles appear to be clump-shaped. The clump-shaped particles of β-$LiAlO_2$ from sample 39A are shown in Fig. 1. The material of sample 65 contained, in addition to the clump-shaped particles, some platelet-shaped particles. The platelets are approximately 4 μm in diameter and 0.5 μm thick, about the same as those of platelets obtained in the past (ANL-77-29, pp. 9-11).

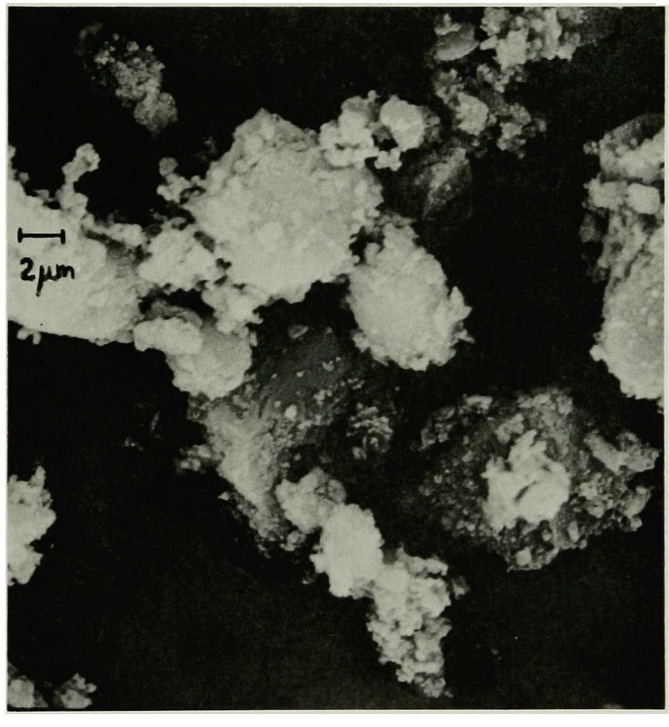

Fig. 1. Clump-Shaped Particles of β-$LiAlO_2$ (3000X)

The experimental conditions and results of the reactions of various types of Al_2O_3 with LiOH, Li_2CO_3, and K_2CO_3 are listed in Table 3. These samples were prepared by mixing powders of Al_2O_3 and LiOH, then adding sufficient Li_2CO_3 and K_2CO_3 (62 mol % Li_2CO_3-38 mol % K_2CO_3) to equal 55 wt % of the sample after formation of $LiAlO_2$. When a sample of this composition was heated to 625 K, the only material that formed was β-$LiAlO_2$; however, heating

Table 2. Preparation of $LiAlO_2$ by the Reaction of Alumina and LiOH

Sample No.	Alumina		Reaction Parameter			
	Phase	Manufacturer (Type)	Temp., K	Time, h	X-ray Analysis	SEM Analysis
27	γ-Al_2O_3	Degussa (C)	595 725	17 1.5	β-$LiAlO_2$	clumps
39A	γ-Al_2O_3[a]	ALCOA (F-1)	625 725	2 4.5	β-$LiAlO_2$	clumps
66A	γ-AlOOH	ALCOA (F-1)	725	1.5	β-$LiAlO_2$ (major) γ-AlOOH (minor)	--[b]
65	γ-AlOOH	ALCOA (F-1)	725	3.5	β-$LiAlO_2$	clumps, platelets

[a] γ-Al_2O_3, obtained by heating γ-AlOOH (ALCOA, F-1) for 68 h at 815 K in air.

[b] SEM analysis not yet completed.

Table 3. Preparation of $LiAlO_2$ by the Reaction of Alumina and LiOH in the Presence of Li_2CO_3-K_2CO_3 Mixtures

Sample No.	Alumina		Reaction Parameter			
	Phase	Manufacturer (Type)	Temp., K	Time, h	X-ray Analysis	SEM Analysis
45	γ-Al_2O_3	Degussa (C)	625	23	β-$LiAlO_2$ γ-Al_2O_3 (poss. minor)	clumps
48	γ-Al_2O_3	Degussa (C)	675	20.5	β-$LiAlO_2$ (major) γ-$LiAlO_2$ (major)	clumps
50	γ-Al_2O_3[a]	ALCOA (F-1)	675	23	β-$LiAlO_2$ (major) γ-$LiAlO_2$ (major) γ-Al_2O_3 (major)	--
61	γ-Al_2O_3[a]	ALCOA (F-1)	725	1.5	γ-$LiAlO_2$ (major) γ-Al_2O_3 (major) β-$LiAlO_2$	clumps
62	γ-Al_2O_3	Degussa (C)	725	1.5	β-$LiAlO_2$ (major) γ-$LiAlO_2$ (major) γ-Al_2O_3 (minor)	clumps
74	γ-Al_2O_3	Degussa (C)	775	1.5	γ-$LiAlO_2$ (major) β-$LiAlO_2$ (poss. minor)	--
75	γ-AlOOH	ALCOA (F-1)	775	1.5	γ-Al_2O_3 (major) γ-AlOOH (medium) γ-$LiAlO_2$ (poss. minor)	clumps
72	γ-Al_2O_3[a]	ALCOA (F-1)	975	1.5	γ-$LiAlO_2$ (major) α-$LiAlO_2$ (minor)	--
73	γ-AlOOH	ALCOA (F-1)	975	1.5	γ-$LiAlO_2$ (major) α-$LiAlO_2$ (major)	clumps

[a] γ-Al_2O_3 obtained by heating γ-AlOOH (ALCOA, F-1) for 68 h at 815 K in air.

a sample mixture at 675 K or greater produced γ-$LiAlO_2$ as well as β-$LiAlO_2$. The γ-Al_2O_3 used in some of the preparations was obtained by dehydrating γ-AlOOH at 815 K for 68 h. In one of these (sample 50), a major phase of γ-Al_2O_3 was still present even after heating the mixture at 675 K for 23 h. On the other hand, unreacted γ-Al_2O_3 was not detected in a mixture (sample 48) containing Degussa γ-Al_2O_3 that was heated at 675 K for 20 h. Thus, it may be concluded that sample 48 reacted more rapidly than sample 50, probably due to the smaller particle size of the γ-Al_2O_3 in the sample 48.

These experiments are the first in which we have been able to synthesize γ-$LiAlO_2$ as a major phase at reaction temperatures of less than 725 K. Generally, γ-$LiAlO_2$ is considered to be the high-temperature form of $LiAlO_2$ (ANL-77-29, pp. 13-18). It is not clear what role the alkali carbonates play in facilitating the formation γ-$LiAlO_2$. We do know, however, that in the absence of carbonates, only β-$LiAlO_2$ is formed by the reaction of LiOH and γ-Al_2O_3 at 725 K or below.

A mixture of γ-AlOOH and a stoichiometric amount of LiOH (sample 75), heated at 775 K for 1.5 h in the presence of alkali carbonates, showed very little reaction to form $LiAlO_2$ (see Table 3). Instead, it appeared that γ-AlOOH was only partially dehydrated. At 975 K, γ-$LiAlO_2$ was the major phase formed in a mixture of LiOH, γ-Al_2O_3, and carbonates (sample 72); however, in a mixture containing γ-AlOOH rather than γ-Al_2O_3 (sample 73), a major phase of α-$LiAlO_2$ was also present after heating at 975 K. The presence of α-$LiAlO_2$ as a major phase in sample 73 and as a minor phase in sample 72 probably reflects a difference in the kinetics of the reaction of LiOH with γ-Al_2O_3 and with γ-AlOOH. It is possible that the larger amount of α-$LiAlO_2$ formed in sample 73 resulted from the reaction of Li_2CO_3 and γ-Al_2O_3 owing to the lower rate of formation of γ-$LiAlO_2$. A kinetic study would be necessary to verify these tentative conclusions.

Scanning electron microscopy (SEM) analysis of selected samples listed in Table 3 showed that the $LiAlO_2$ particles were generally clump-shaped. The samples containing γ-$LiAlO_2$ showed no clear evidence of the formation of the bipyramidal-shaped particles which are usually associated with the formation of γ-$LiAlO_2$ at high temperatures (ANL-77-29, p. 16). It appears, therefore, that γ-$LiAlO_2$ can now be obtained in several particle shapes. (The formation of rod-shaped particles of γ-$LiAlO_2$ is discussed in subsection B below.)

Thermal stability studies (ANL-77-29, pp. 13-18) have previously indicated that γ-$LiAlO_2$ is the most stable allotropic form of $LiAlO_2$ for molten-carbonate fuel-cell applications. Therefore, if γ-$LiAlO_2$ of small particle size and appropriate shape can be prepared by practical methods from inexpensive alumina, we believe that most of the problems of $LiAlO_2$ synthesis will have been solved. The fact that a major phase of γ-$LiAlO_2$ was obtained by heating a physical mixture of LiOH, Li_2CO_3, K_2CO_3 and γ-Al_2O_3 (Degussa) at 775 K is encouraging because we believe that preparation of high-surface area γ-$LiAlO_2$ requires a low-temperature synthesis. Future experiments will be directed toward optimizing the reactant compositions, reaction time, and temperature that are required to produce high-surface-area γ-$LiAlO_2$.

B. Physical Stability of $LiAlO_2$

1. Introduction

A knowledge of the thermal stability of $LiAlO_2$ is necessary in understanding and improving tile behavior because the electrolyte-retention properties of a tile and its strength are dependent both upon the allotropic form of $LiAlO_2$ and upon the size, shape, and surface area of the $LiAlO_2$ particles within the tile. A phase transformation from α-$LiAlO_2$ to the β- or γ-allotrope produces a volume change in the tile (the densities of the α-, β-, and γ-allotropes are 3401,[1] 2610,[2] and 2615[3] kg/m^3, respectively). This volume change alters the pore structure and thereby changes the electrolyte-retention properties of the tile. Particle growth, which also produces significant changes in the pore structure of the tile, adversely affects cell performance. These changes in the pore structure and in the shape and size of the $LiAlO_2$ particles may also reduce tile strength.

The transformation of α-$LiAlO_2$ to γ-$LiAlO_2$ has been studied extensively.[1,4-9] Lehmann and Hesselbarth[4] concluded that in air α-$LiAlO_2$ is partially converted to γ-$LiAlO_2$ at temperatures greater than 875 K but rapid and complete conversion occurs at 1175 K. Semenov[5] noted that in air the conversion of α-$LiAlO_2$ to γ-$LiAlO_2$ is accelerated by the presence of Li_2CO_3 or Li_2SO_4. Gal *et al.*[6] found that in the presence of Li_2CO_3, α-$LiAlO_2$ transforms rapidly to γ-$LiAlO_2$ at 1125 K in air, in general agreement with Semenov; however, they found that in CO_2 the effect of Li_2CO_3 is counteracted and transformation of α- to γ-$LiAlO_2$ required a temperature of 1225 K.

Chang *et al.*[7] noted that heating at 985 K in air for 72 h had no effect on β-$LiAlO_2$. Fischer[2] reported that in air β-$LiAlO_2$ transformed to γ-$LiAlO_2$ at 1175 K but did not give the time required. Our previous work showed that at 925 K β-$LiAlO_2$ mixed with 55 wt % Li_2CO_3-K_2CO_3 (molar ratio, 0.62/0.38) remained stable for 2400 h in air and in $H_2/CO_2/H_2O$ (ANL-77-79, p. 8) and for 530 h in CO_2/air (ANL-77-56, p. 5); however, a mixture of the same composition transformed to γ-$LiAlO_2$ in less than 100 h at 975 K in CO_2 (ANL-77-29, p. 15).

To achieve optimum performance of fuel cells for long lifetimes, it is essential to determine the range of temperatures in which the thermal stability of $LiAlO_2$ is maintained in the presence of carbonate in the gas environments found in the fuel cell. Moreover, because an interdependence exists between the thermal stability of the three allotropes of $LiAlO_2$ and the environment in which they exist, the dependence of the thermal stability of each allotropic form on temperature, carbonate concentration, and gas environment must be determined. The operating temperature of the molten-carbonate fuel cell will be in the range from 870 to 970 K; however, temperature gradients must be expected within the cells, and from cell to cell in the cell stacks. Therefore, we are concerned with the thermal stability of $LiAlO_2$ not only at normal operating temperatures but at higher temperatures (970-1190 K). The gas environments present in the fuel cell are CO_2 (at the cathode), $H_2/CO_2/H_2O$ (at the anode), and air (at the wet seal); hence, the thermal behavior of the three allotropic forms must be determined in each of these environs.

The purpose of our work, then, is to define the parameters important to maintaining particle form, size, shape, and surface area by means of short-term and then long-term tests in the temperature range from 870 to 1190 K. The parameters of interest are the presence or absence of alkali carbonate, the temperature, and the gas composition. Products are identified by X-ray diffraction to determine allotropic form and are examined by scanning electron microscopy to establish changes in particle morphology. Surface areas will be determined by the BET method, if such measurements are judged to be useful.

2. Results and Discussion

Table 4 presents a summary of the results of thermal stability experiments in which powders of $LiAlO_2$ or a mixture of $LiAlO_2$ and alkali carbonate, contained in gold crucibles, were heated in air. The final $LiAlO_2$ products (last column, Table 4) were identified by X-ray powder diffraction; the terms minor and major signify the amounts of the phases present (25-45% and 45-95%, respectively). Transformation of α-$LiAlO_2$ to γ-$LiAlO_2$ occurred in 15 h at 970 K in air in the presence of alkali carbonates; however, in the absence of carbonates, α-$LiAlO_2$ remained stable to 1125 K but decomposed at 1230 K, as indicated by the formation of $LiAl_5O_8$ and γ-Al_2O_3. In the presence of carbonates, β-$LiAlO_2$ remained stable for 39 h at 960 K, but at 1030 K it was completely transformed to γ-$LiAlO_2$ in 23 h. In the absence of carbonates, β-$LiAlO_2$ was transformed to γ-$LiAlO_2$ after 24 h at 1110 K but was unchanged after 23 h at 1030 K.

If high pressure is applied, γ-$LiAlO_2$ transforms to α-$LiAlO_2$;[7] but at normal pressures, we have not observed transformation of γ-$LiAlO_2$ to either α- or β-$LiAlO_2$. After heating of a mixture of γ-$LiAlO_2$ and alkali carbonate at 1110 K for 24 h in air, the γ-$LiAlO_2$ decomposed to form β-Li_5AlO_4, the high-temperature allotrope of this compound. The amount of β-Li_5AlO_4 detected varied among samples (very minor to major); this variation is attributed to sample location in the furnace. The other product of the decomposition may be Al_2O_3, although no Al_2O_3 was detected by X-ray analysis, possibly due to effects of crystallite size.

A scanning electron micrograph of γ-$LiAlO_2$ after heat treatment at 1110 K in air in the presence of carbonates revealed that particle growth had occurred, as indicated by the presence of large, rounded octahedra (Fig. 2) which were three to fifteen times larger than the starting material. The rodlike morphology of β-$LiAlO_2$ was maintained during phase transformation to γ-$LiAlO_2$, when the transformation occurred in the absence of carbonates. A scanning electron micrograph of the rod-shaped γ-$LiAlO_2$ is presented in Fig. 3.

These results indicate that considerably more data are needed on the thermal stability of $LiAlO_2$. Our studies of the thermal stability of $LiAlO_2$ in the presence of alkali carbonates will be continued, with emphasis on the effects of CO_2 and $H_2/CO_2/H_2O$ gaseous environments.

Table 4. Thermal Stability of $LiAlO_2$

Initial $LiAlO_2$ Phase	Environment	Temp., K	Time, h	Products
α-$LiAlO_2$	air, carbonates	970	15	γ-$LiAlO_2$, α-$LiAlO_2$ (minor)
α-$LiAlO_2$	air	970	15	α-$LiAlO_2$
α-$LiAlO_2$	air	1125	64	α-$LiAlO_2$
α-$LiAlO_2$	air	1230	41.5	γ-$LiAlO_2$, γ-Al_2O_3 $LiAl_5O_8$
β-$LiAlO_2$	air, carbonates	960	39	β-$LiAlO_2$
β-$LiAlO_2$	air, carbonates	1030	23	γ-$LiAlO_2$
β-$LiAlO_2$	air	960	39	β-$LiAlO_2$
β-$LiAlO_2$	air	1030	23	β-$LiAlO_2$
β-$LiAlO_2$	air	1110	24	γ-$LiAlO_2$, β-$LiAlO_2$ (minor)
β-$LiAlO_2$	air	1210	63	γ-$LiAlO_2$[a]
γ-$LiAlO_2$	air, carbonates	1110	24	γ-$LiAlO_2$[b], β-Li_5AlO_4 (very minor to major)
γ-$LiAlO_2$	air	1260	5.5	γ-$LiAlO_2$

[a] Scanning electron micrograph indicated rods similar to those of β-$LiAlO_2$ (Fig. 3).

[b] Scanning electron micrograph indicated large rounded octahedra (Fig. 2).

C. Chemical Stability of $LiAlO_2$

A knowledge of the chemical stability of the three allotropes of $LiAlO_2$ in various media is needed in the development of analytical procedures for separating $LiAlO_2$ from carbonates and isolating it in pure, unchanged form. Studies of the chemical stability of $LiAlO_2$ in water by Lejus[9] showed that α-$LiAlO_2$ does not hydrolyze in boiling water or in acid, whereas γ-$LiAlO_2$ reacts with water in a few hours via a two-step process. The first step is the rapid formation of an intermediate "H" phase; the second step is much slower and produces $Al_2O_3 \cdot 3H_2O$. No information on the chemical stability of β-$LiAlO_2$ in water has been found in the literature.

An analytical procedure for isolating $LiAlO_2$ from alkali carbonates, which avoided the possibility of reaction of $LiAlO_2$ with water was previously reported (ANL-77-79, pp. 8 and 20). This procedure has now been modified to accommodate considerably larger samples with no increase in volume of solution. In the original procedure, 100 mg of a mixture of $LiAlO_2$

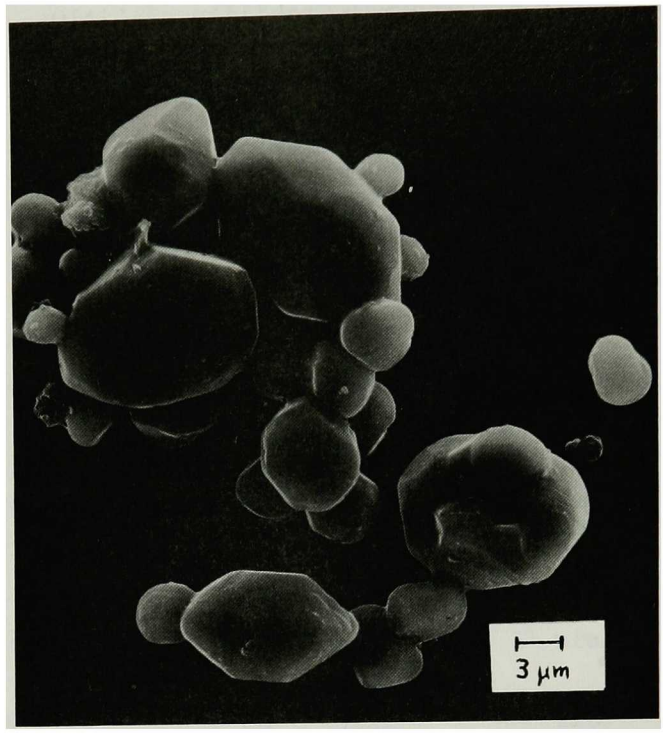

Fig. 2. Scanning Electron Micrograph of γ-$LiAlO_2$ After Heat Treatment at 1110 K in Presence of Alkali Carbonates (2000X).

and alkali carbonate was added to 100 mL of 70 vol % glacial acetic acid/30 vol % acetic anhydride. In the revised procedure, ~10-20 g of a mixture of $LiAlO_2$ and alkali carbonate is added to ~100 mL of a cooled (ice-bath) solution of 38 vol % glacial acetic acid/62 vol % acetic anhydride. The increased amount of acetic anhydride doubles the capacity for reaction with water. The solution is cooled to avoid undesirable side reactions. The solid $LiAlO_2$ is separated by centrifugation from the solution, which contains the dissolved alkali acetates; it is then washed several times with methanol to remove the acetate salts completely. The method has been tested on samples of α-, β-, and γ-$LiAlO_2$; all three materials can be separated from carbonates and hydrolysis products in unchanged allotropic form, as shown in Table 5. Yields are typically 80-90%; losses are believed to result from problems in handling the small-particle-size material.

The relative reactivities of the three allotropic forms of $LiAlO_2$ to water and to 6*M* HCl were determined, and these results are included in Table 5. The treatment of α-$LiAlO_2$ with water produced only α-$LiAlO_2$, in agreement with the results of Lejus.[9] The product(s) of the reaction between water and γ-$LiAlO_2$ were $LiH(AlO_2)_2 \cdot 5H_2O$ and/or $Li_2Al_2O_4 \cdot yH_2O$,*

*The X-ray patterns of these two compounds could not be differentiated.

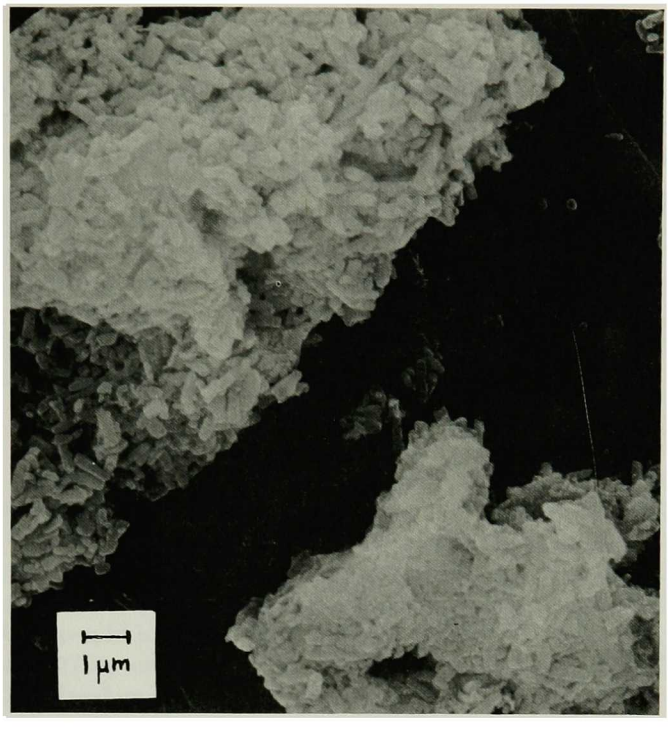

Fig. 3. Scanning Electron Micrograph of γ-$LiAlO_2$ Formed During Heat Treatment of β-$LiAlO_2$ at 1210 K in Absence of Alkali Carbonates (6000X)

which may correspond to Lejus' "H" phase. Further hydrolysis was not detected after 4 h. The treatment of β-$LiAlO_2$ with water yielded β-$LiAlO_2$ after 4 h but some $Li_2AlO_4 \cdot yH_2O$ and/or $LiH(AlO_2)_2 \cdot 5H_2O$ after 168 h.

The solid product isolated from reaction of 6*M* HCl and γ-$LiAlO_2$ in the presence of carbonate was $AlCl_3 \cdot 6H_2O$. On the basis of a previous study, which showed that the reaction between 6*M* HCl and γ-Al_2O_3 yields $AlCl_3 \cdot 6H_2O$, we have concluded that the reaction between aqueous HCl and γ-$LiAlO_2$ proceeds first by hydrolysis of γ-$LiAlO_2$ to form γ-Al_2O_3, which then reacts with HCl to form $AlCl_3 \cdot 6H_2O$. A very minor amount of $LiH(AlO_2)_2 \cdot 5H_2O$ was formed from the reaction between α-$LiAlO_2$ and 6*M* HCl. (The reaction product may have resulted from an impurity in the α-$LiAlO_2$ sample.) When a mixture of β-$LiAlO_2$ and alkali carbonates was added to 6*M* HCl, the sample completely dissolved. (The large excess of acid used precluded recovery of the reaction products.) From these experiments, we have concluded that aqueous HCl is unsuitable for use in isolating $LiAlO_2$.

In summary, we have devised an improved procedure for isolating $LiAlO_2$ from alkali carbonate using 38 vol % glacial acetic acid/62 vol % acetic anhydride. We plan to refine this separation technique further and to complete the study of the hydrolysis behavior of $LiAlO_2$.

Table 5. Chemical Stability of $LiAlO_2$ at Ambient Temperature

Expt. No.	Initial $LiAlO_2$ Phase	Environment	Time, h	Final Product[a]
4	α-$LiAlO_2$	H_2O	720	α-$LiAlO_2$
5	β-$LiAlO_2$	H_2O	168	β-$LiAlO_2$ (major), $Li_2Al_2O_4 \cdot yH_2O$ and/or $LiH(AlO_2)_2 \cdot 5H_2O$ (minor)
6	γ-$LiAlO_2$	H_2O	4	$Li_2Al_2O_4 \cdot yH_2O$ and/or $LiH(AlO_2)_2 \cdot 5H_2O$
1	α-$LiAlO_2$[b]	38 vol % CH_3COOH 62 vol % $(CH_3CO)_2O$	4	α-$LiAlO_2$
2	β-$LiAlO_2$[b]	38 vol % CH_3COOH 62 vol % $(CH_3CO)_2O$	4	β-$LiAlO_2$
3	γ-$LiAlO_2$[b]	38 vol % CH_3COOH 62 vol % $(CH_3CO)_2O$	4	γ-$LiAlO_2$
7	α-$LiAlO_2$[b]	6*M* HCl	4	α-$LiAlO_2$ (major), $LiH(AlO_2)_2 \cdot 5H_2O$ (very minor)
8	β-$LiAlO_2$[b]	6*M* HCl	0.2	sample dissolved
9	γ-$LiAlO_2$[b]	6*M* HCl	4	$AlCl_3 \cdot 6H_2O$

[a] From X-ray diffraction analyses.

[b] Alkali carbonates present.

III. CELL TESTING

The primary objective of cell testing at ANL is to understand and control properties of the cell components and the changes in these properties during cell operation. The components that have received particular emphasis are the electrolyte tile and the wet-seal area of the cell housings. Our previous work (ANL-77-79, pp. 9-12) has shown that the cell performance is affected by the type of $LiAlO_2$ particles used to retain the alkali carbonates in the electrolyte tile. Rod-shaped β-$LiAlO_2$ particles of relatively uniform size and shape ($\sim$4 μm long, $\sim$0.7 μm in diameter) were ineffective in retaining the alkali carbonates, and cells utilizing this type of $LiAlO_2$ exhibited high polarization. Particles of an ill-defined, clump shape were more effective in retaining alkali carbonates, and cells that utilized this type of $LiAlO_2$ have delivered the best performance of any cells tested at ANL.

The effects of $LiAlO_2$ particle morphology on cell performance were investigated further during the past quarter. Electrolyte tiles containing mixtures of the rod-shaped and clump-shaped particles were tested in fuel cells. A direct correlation was observed between cell performance and the relative proportions of each morphology in the electrolyte tile. As the ratio of clump-shaped α-$LiAlO_2$ to rod-shaped β-$LiAlO_2$ was increased, the cell performance improved. The effects of increasing the amount of the alkali carbonates in the electrolyte tile (from 55 to 60 wt %) were also investigated. A substantial reduction ($\sim$30%) in ohmic polarization was observed, without a significant change in other sources of polarization. An electrolyte tile containing clump-shaped β-$LiAlO_2$ prepared from low-cost alumina was also tested in a cell. The performance of the cell was poor, due to reactant-gas cross-leakage through the electrolyte tile. The cross-leakage occurred at large voids in the tile caused by poor retention of the alkali carbonates. Although retention of the alkali carbonates by this type of $LiAlO_2$ was poor, it is possible that this characteristic was due to the synthesis procedure and not to the type of alumina used in the synthesis.

The method of wet-seal protection developed previously at ANL (ANL-77-79, pp. 12-14) has been tested with another set of cell housings. The aluminizing coating in these housings has been extended to cover areas near the wet seal, which were not coated previously and which showed significant corrosion in earlier cell housings. (The anode and cathode housings were both coated in the same manner.) The new housings have accumulated 663 h of cell operation, in two separate cell assemblies, with satisfactory corrosion protection.

Operation of the CS-series of cells was continued with Cells CS-9 through CS-12. Cells CS-9 and CS-11 were operated to test electrolyte tiles containing mixtures of rod-shaped β-$LiAlO_2$ and clump-shaped α-$LiAlO_2$ as the support matrix material. Cell CS-10 was operated to test the effect on cell performance of increasing the amount of alkali carbonates in the electrolyte tile and Cell CS-12, to test $LiAlO_2$ which was prepared from low-cost alumina. Characteristics of these cells and some cells operated previously are summarized in Table 6. The anode gas composition used in cell testing was 80% H_2, 20% CO_2, to which moisture (dew point 298 K) was added. The cathode gas composition was 14.5% O_2, 28.0% CO_2, 57.5% N_2, which simulates 70% air, 30% CO_2.

Table 6. Characteristics of Selected Cells in the CS-Series

	CS-4	CS-7	CS-9	CS-10	CS-11	CS-12
Electrolyte Tile						
Thickness, cm	0.22-0.24	0.19-0.21	0.21-0.22	0.20-0.21	0.20-0.21	0.20-0.22
Alkali Carbonates, wt %	55	55	55	60	55	55
$LiAlO_2$ Morphology	rods	clumps	clumps & rods	clumps	clumps & rods	clumps
Weight Ratio of $LiAlO_2$ Particles (clumps:rods)	0:1	1:0	1:1	1:0	4:1	1:0
Electrodes						
Anode	a	c	c	d	c	d
Cathode	b	b	b	b	b	b
Area (all cells): 28.6 cm^2						
Cell Resistance, mΩ	32	26	32	18	28	44

a: Gould 309-144-3 compressed to 0.033 cm.
b: Union Carbide 306-24-30B.
c: Gould 309-144-3 compressed to 0.043 cm.
d: Union Carbide 306-24-30C.

The performance of Cells CS-4, CS-7, CS-9, and CS-11 is compared in Fig. 4. These cells constitute a series in which the major variable is the type of $LiAlO_2$ used to prepare the electrolyte tile. The method of $LiAlO_2$ preparation for each of thses cells is summarized in Table 1, Section II of this report. The data in Fig. 4 clearly show that cell performance is related to the amount of each morphology present in the electrolyte tile.

The performance of CS-7 is clearly the best, and is typical of cells with electrolyte tiles containing only clump-shaped α-$LiAlO_2$ as the support matrix material. The performance of Cell CS-4 is the poorest, and is typical of cells with electrolyte tiles containing only rod-shaped β-$LiAlO_2$. When a mixture of the two morphologies is used, intermediate performance is obtained (Cells CS-9 and CS-11). In the tile of Cell CS-9, the two morphologies were in approximately equal proportions, whereas in Cell CS-11, the morphologies were in a ratio of approximately 4:1 (clumps:rods). As can be seen in Fig. 4, the performance of Cell CS-11 is closer to that of Cell CS-7 than is the performance of Cell CS-9. Thus, cell performance can be directly correlated with the relative amounts of the two morphologies in the electrolyte tile.

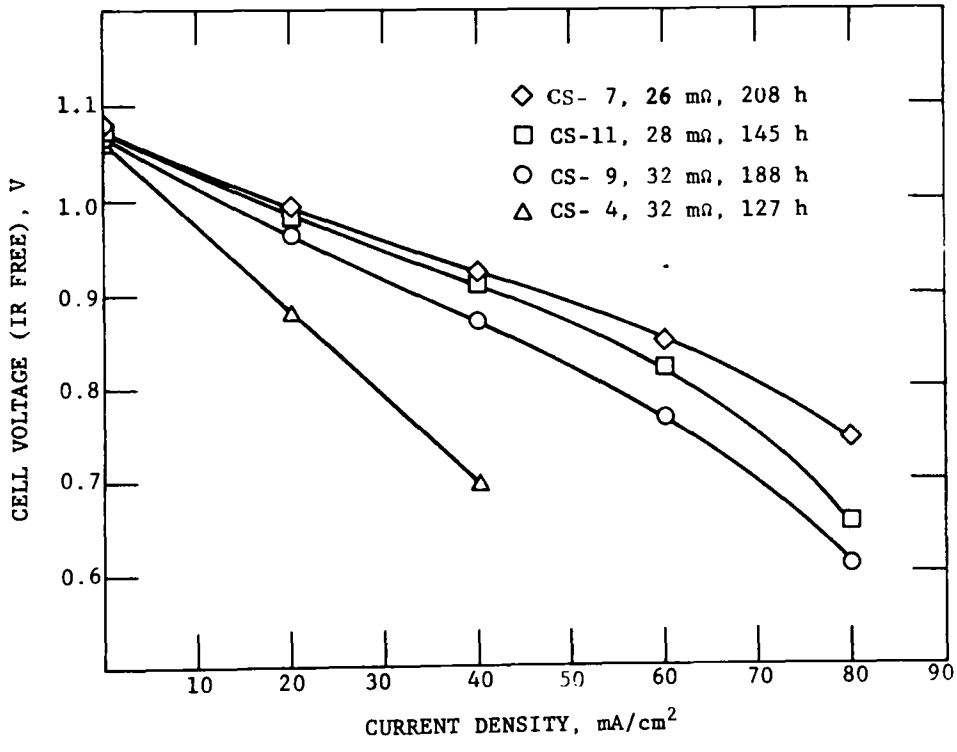

Fig. 4. Comparison of Performance of Cells CS-4, CS-7, CS-9 and CS-11 (temperature, 925 K; gas flow to each electrode, 3A; electrode areas, 28.6 cm^2)

These results clearly indicate that some characteristics of the clump-shaped α-$LiAlO_2$ improve fuel cell performance, while some characteristics of the rod-shaped β-$LiAlO_2$ adversely affect cell performance. Examination by SEM indicates that the clump-shaped α-$LiAlO_2$ probably has a much higher surface area than the rod-shaped β-$LiAlO_2$. Particles with the clump morphology appear to possess a higher degree of internal microporosity, perhaps resulting from the agglomeration of smaller particles to form the observed clump-shaped morphology. Rod-shaped particles, however, possess no apparent internal microporosity, and their overall size may be too large to provide good electrolyte retention.

Other characteristics of the clump-shaped α-$LiAlO_2$ may adversely affect cell performance, however. Previous studies (ANL-77-29, p. 15) have shown that α-$LiAlO_2$ was transformed to γ-$LiAlO_2$ under fuel-cell operating conditions. This transformation is accompanied by a change in the density of the $LiAlO_2$, and in its particle shape and size. These changes in density and particle morphology can be expected to disrupt the distribution of alkali carbonates in the cell, thereby affecting cell performance. Efforts are being made, under the electrolyte development task, to synthesize higher-surface-area γ-$LiAlO_2$. Use of high-surface-area γ-$LiAlO_2$ in the electrolyte tile is expected to mitigate the problem of phase transformation, while maintaining the characteristics necessary for the retention of alkali carbonates.

In Fig. 5 the performance characteristics of Cells CS-7 and CS-10 are compared. The major variable in the construction of these two cells is the amount of alkali carbonates in the electrolyte tile: 60 wt % carbonates in CS-10 and 55 wt % carbonates in CS-7. The support matrices for both cells

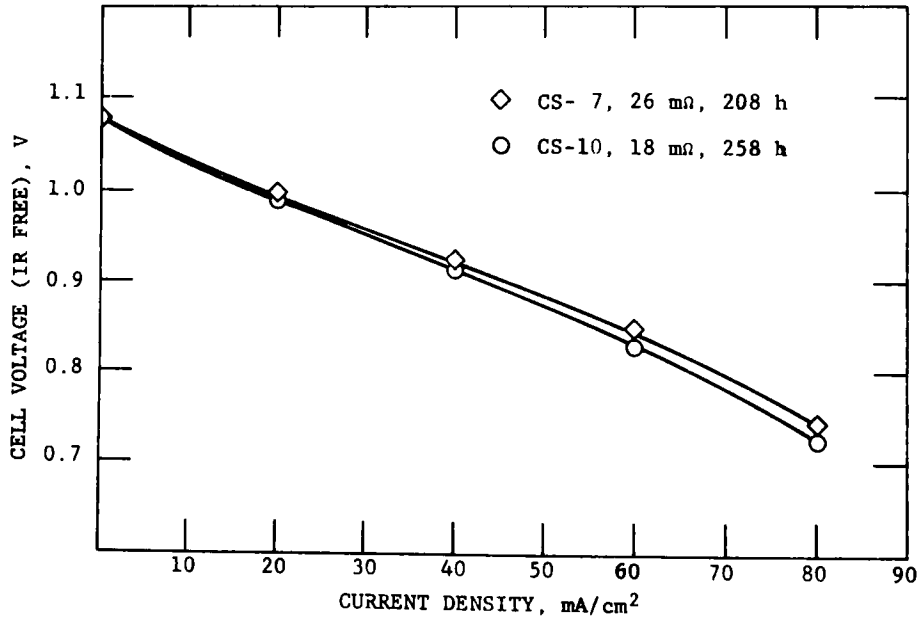

Fig. 5. Comparison of Performance of Cells CS-7 and CS-10 (temperature, 925 K; gas flow to each electrode, 3A; electrode areas, 28.6 cm^2)

were clump-shaped α-$LiAlO_2$ particles. Cell CS-10 had a resistance of 18 mΩ, and Cell CS-7 had a resistance of 26 mΩ. Although the IR-free voltage of Cell CS-10 is slightly lower than that of Cell CS-7, the difference is probably not significant. Thus, a substantial reduction in ohmic polarization was realized by increasing the amount of alkali carbonates in the electrolyte tile. Significant increases in other sources of polarization were not observed, as might be expected if the increase in electrolyte content had led to electrode flooding.

In Fig. 6, the performance of Cell CS-12 is compared with that of Cell CS-7, which may be considered to be a baseline performance cell. Cell CS-12 was constructed to test a clump-shaped form of β-$LiAlO_2$ (sample 39A, Table 2) prepared from a low-cost alumina. The lower performance of Cell CS-12

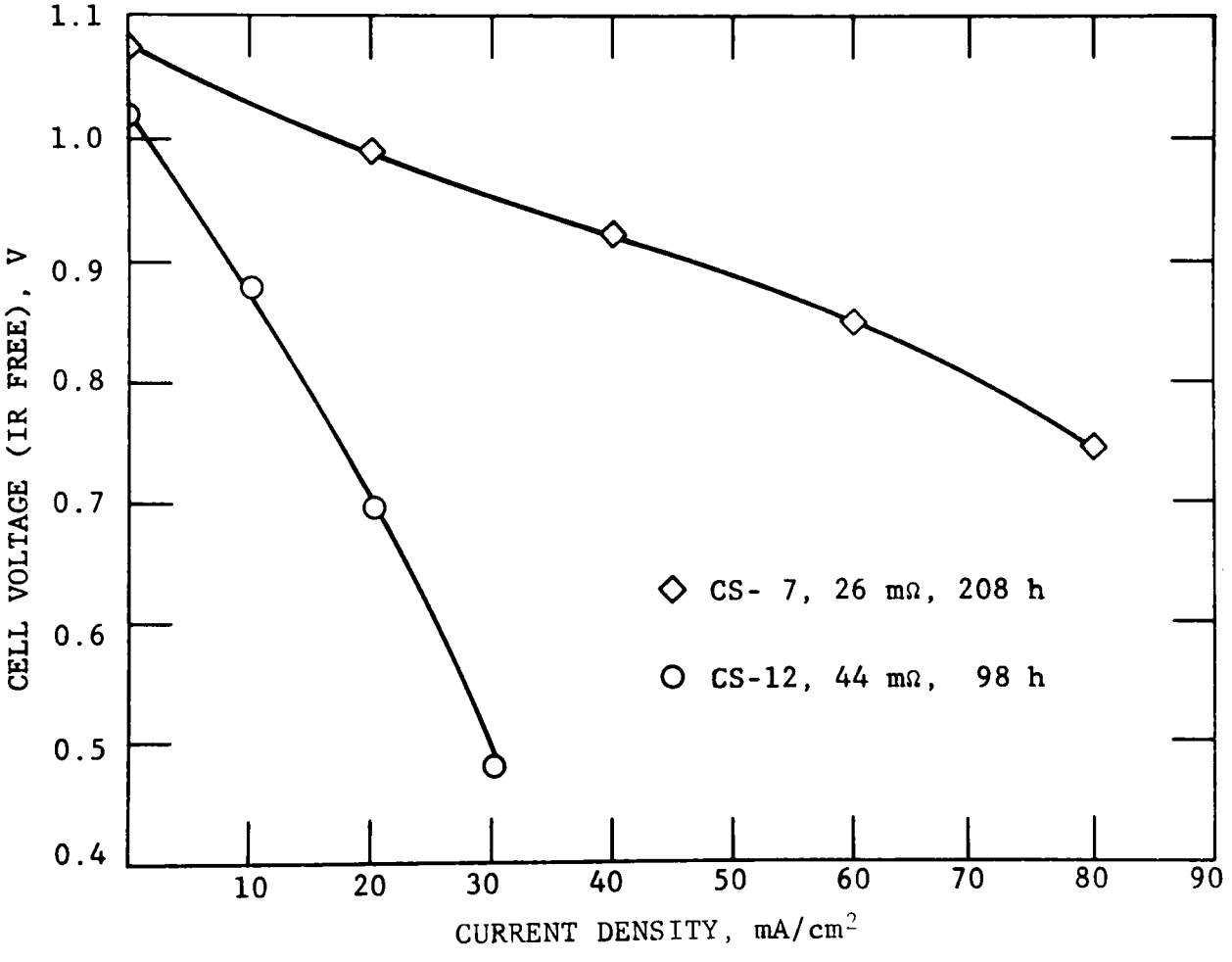

Fig. 6. Comparison of Performance of Cells CS-7 and CS-12 (temperature, 925 K; gas flow to each electrode, 3A; electrode areas, 28.6 cm^2)

was a result of reactant gas cross-leakage through the electrolyte tile. Cell CS-12 is the first cell in which the occurrence of a significant cross-leakage of reactant gases has been clearly established. Its open-circuit voltage was ∿60 mV lower than other cells in the CS-series. Also, the open-circuit voltage was decreased by imposing a small differential pressure of <0.8 kPa (3 in. of water) across the electrolyte tile. Since only the cathode gas stream contains nitrogen, analysis of the anode effluent gas stream for N_2 can be used to detect cross-leakage. Gas chromatographic analyses of the anode effluent gas stream of Cell CS-12 indicated 4.5% N_2 with no pressure differential across the electrolyte tile and 26.0% N_2 with a pressure differential of 2.0 kPa (8 in. of water). For comparison, when similar measurements were made on Cell CS-7, <0.5% N_2 was detected, and the amount detected was virtually independent of the pressure differential across the electrolyte tile, up to about 2.0 kPa. Thus, reactant gas cross-leakage can be detected, during cell operation, by analyzing the anode effluent gas stream for N_2, and by observing the effect of a pressure differential across the tile on the open-circuit voltage.

Post-test examination of Cell CS-12 also indicated that the $LiAlO_2$ used in the electrolyte tile was ineffective in retaining the alkali carbonates. Gross deformation of the electrolyte tile was observed, a characteristic that is typical of tiles with poor retention properties. Creeping of alkali carbonates around the cell housings was also very apparent. Since the $LiAlO_2$ used in the tile of Cell CS-12 was the first prepared from a low-cost alumina, the poor retention properties should not necessarily be attributed to the alumina used in this synthesis. We plan to test other types of $LiAlO_2$ which have been synthesized from low-cost aluminas.

Next quarter, use of the round CS-series cells will be discontinued, and tests will be conducted in square cells with well-controlled gas and current distributions. The design of the square cells should also provide a better support for the current collector and hence result in lower IR losses and longer life for the cells. A significant improvement in both short- and long-term cell performance is expected from these new cells.

REFERENCES

1. M. Marezio and J. P. Remeika, J. Chem. Phys. 44, 3143 (1966).

2. A. K. Fischer, Inorg. Chem. 16, 974 (1977).

3. M. Marezio, Acta Cryst. 19, 396 (1965).

4. H. A. Lehmann and H. Hesselbarth, Z. Anorg. Allgem. Chem. 313, 117 (1961).

5. N. N. Semenov, Izv. Sib. Otd. Akad. Nauk SSSR Ser. Khim. Nauk 1, 156 (1967).

6. S. Gal, K. Tomor, E. Pungor, G. Sooki-Toth and P. Horvath, J. Thermal Anal. 9, 241 (1976).

7. C. H. Chang and J. L. Margrave, J. Am. Chem. Soc. 90, 2020 (1968).

8. A. M. Lejus and R. Collongues, Compt. Rend. 254, 2005 (1962).

9. A. M. Lejus, Rev. Hautes Temp. Refract. 1, 72 (1964).

Distribution for ANL-78-16

Internal:

E. G. Pewitt
J. P. Ackerman (25)
E. M. Bohn
L. Burris
F. A. Cafasso
L. Cuba
P. A. Finn
J. Harmon
R. O. Ivins
G. M. Kesser
K. Kinoshita
A. Melton
P. A. Nelson
J. W. Sim
R. K. Steunenberg
R. Swaroop
A. D. Tevebaugh
D. S. Webster
A. B. Krisciunas
ANL Contract Copy
ANL Libraries (5)
TIS Files (6)

External:

DOE-TIC, for distribution per UC-93 (171)
Manager, Chicago Operations Office
Chief, Chicago Patent Group
President, Argonne Universities Association
Chemical Engineering Division Review Committee:
- C. B. Alcock, U. Toronto
- R. C. Axtmann, Princeton U.
- R. E. Balzhiser, Electric Power Research Inst.
- J. T. Banchero, U. Notre Dame
- T. Cole, Ford Motor Co.
- P. W. Gilles, U. Kansas
- R. I. Newman, Allied Chemical Corp.
- G. M. Rosenblatt, Pennsylvania State U.

T. R. Beck, Electrochemical Technology Corp., Seattle
K. Blurton, Inst. of Gas Technology, Chicago
A. Borucka, Borucka Research Co., Livingston, NJ
D. Chatterji, General Electric Co., Schenectady
G. Ciprios, Exxon Research and Engineering Co., Linden, NJ
L. M. Ferris, Oak Ridge National Lab.
A. P. Fickett, Electric Power Research Inst.
J. W. Harrison, General Electric Co., Wilmington, MA
J. Huff, U. S. Army Mobility Equipment R&D Center
J. M. King, United Technology Corp.
A. R. Landgrebe, Div. of Energy Storage Systems, USDOE
L. R. Lawrence, Div. of Conservation Research and Technology, USDOE (3)
J. J. Rasmussen, Montana Energy and MHD Research Inst.
R. Roberts, The Mitre Corp.
W. E. Wallace, Jr., Morgantown Energy Research Center
E. Yeager, Case Western Reserve U.